

## INTERACTION OF SODIUM VAPOR AND GRAPHITE STUDIED BY THERMOGRAVIMETRIC ANALYSIS

Z. Wang<sup>1,3</sup>, A.P. Ratvik<sup>2</sup>, E. Skybakmoen<sup>2</sup> and T. Grande<sup>1</sup>

<sup>1</sup>Department of Materials Science and Engineering, Norwegian University of Science and Technology, NO-7491 Trondheim, Norway

<sup>2</sup>SINTEF Materials and Chemistry, NO-7465 Trondheim, Norway

<sup>3</sup>Corresponding author: [zhaohui.wang@material.ntnu.no](mailto:zhaohui.wang@material.ntnu.no)

Keywords: Aluminum Electrolysis, Graphite, Thermogravimetry, Sodium Diffusion, DFT Calculation

### Abstract

Intercalation of sodium in carbon materials is of paramount importance for the Hall-Héroult process. The interaction of sodium and graphite has been investigated for decades, but despite considerable efforts, the transport and nature of sodium in carbon materials are still poorly understood. Here we report on a study of the interaction between graphite and sodium vapor by thermogravimetric analysis. A graphitized carbon material was exposed to sodium vapor, and the equilibration of sodium uptake in the carbon material was monitored. The kinetics of the sodium uptake is discussed with respect to surface adsorption, bulk diffusion and the solid solubility of sodium in graphite. The kinetics of the reaction was analyzed with support from finite element method simulations. Finally, recent density functional theory simulations of sodium intercalation compounds are presented, demonstrating the low thermodynamic stability of such sodium intercalation compounds reflecting the low reactivity of sodium with carbon.

### Introduction

Sodium plays an important role in the degradation of the entire cathode lining in the Hall-Héroult reduction cell in aluminum production, not only the carbon cathode, but also the refractory and the sideling [1-4]. During the electrolysis sodium will be produced by the following reactions [5]:



or



The vapor pressure of sodium above aluminum in contact with bath depends on the bath chemistry and temperature. The vapor pressure is around 0.02 to 0.03 bar at 960 °C [6]. Sodium will inevitably infiltrate or react the cathode carbon materials. The interaction of sodium and carbon cathode materials initializes the degradation of the whole lining.

Sodium in carbon has been investigated for decades [5, 7-11], but despite considerable efforts, the transport and nature of sodium in carbon materials are still poorly understood. Several methods have been applied to derive the diffusion coefficient of sodium in carbon. The direct reaction between sodium and carbon by the Rapoport test was first published in 1957 [12] with further fitting by Bessel function. Sodium diffusion has also been investigated by measurement of the sodium penetration front as a series of time and, fitting by Fick's 2<sup>nd</sup> law with a semi-infinite model [5]. In addition, sodium content in carbon could be obtained by leaching and back titration after certain times of sodium exposure, and fitting by semi-infinite body, the diffusion coefficient could

also be derived [13]. The reported diffusion coefficients are, however, scattered by several orders of magnitude [7, 8, 13-16]. The data are also difficult to compare due to the influence of the testing conditions, like bath chemistry, external electronic field and/or external stress. It is, however, observed that sodium expansion is a function of current density and that the cathode contracts to its original state when current is shut off. Hence, the expansion is believed to be due to the activity of sodium at the bath electrolyte interphase and the present work is initiated to explore this phenomena in more detail.

The present work provides a new method for determining the diffusion coefficient of sodium vapor in carbon materials through a thermogravimetric relaxation method. During the test, thermogravimetric relaxation curves are obtained, showing sodium uptake over time until saturation. The sodium uptake is modeled by FEM simulation to determine a diffusion coefficient for sodium in carbon. The relaxation curves were also studied using the BET isotherm theory, previously used to describe the saturation of sodium in carbon materials [9]. Finally, the sodium interaction with carbon is discussed with support from recent studies of sodium intercalation compounds by density functional theory (DFT) [17].

### Experimental

A schematic illustration of the experimental setup of the thermogravimetric apparatus, including the furnace with two temperatures zones, is shown in Figure 1. The apparatus has previously been used for absorption tests of metallic sodium in carbon cathode materials [9]. The set-up was modified to enable better vacuum control. Before the experiments were initiated, the system was evacuated to 10<sup>-2</sup> mbar at least 3 times, flushing the furnace with Ar in between. Around 200 mbar argon gas was filled into the reactor during the test in order to avoid boiling of sodium in zone 2. The carbon samples were heated up to the experimental temperature before sodium exposure to remove volatile species in the carbon material. Sodium at the bottom of the reactor was then heated up to a specific temperature. A furnace with two heating zones was used to keep the carbon sample temperature higher than the sodium temperature in order to avoid condensation of sodium. The vapor pressure of sodium was determined by the temperature in zone 2. The sodium vapor in the reactor interacted with the carbon cylinder sample attached by a wire to an electronic balance (WXSS204, Mettler Toledo). The weight change of the carbon sample was recorded by the balance. In addition to the weight gain, temperature and pressure of the system were recorded as a function of time.

The carbon material used in the present work was isotropic graphite (IG-15, Toyo Tanso Co., LTD.). The samples were

shaped in a cylinder with 2 cm diameter and 3 cm height. The sample was attached to the balance by a Ni-Cr alloy wire (BRIGHTRAY<sup>®</sup> alloy C, Special Metals), which showed the best performance with respect to the reaction with the sodium vapor. Ni wire used in previous work [9] could not be used due to the introduction of noise in the weight signal. A blank experiment without carbon was also carried out to estimate the mass gain due to interaction between the wire and the sodium gas.

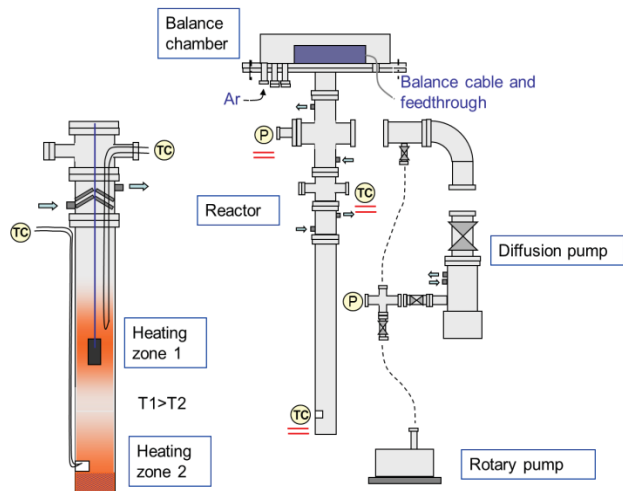


Figure 1. Schematic drawing of the experimental setup of thermogravimetric apparatus together with a section drawing of the reactor.

Several experiments were carried out in order to optimize the experimental protocol. The results of only two of the thermogravimetric experiments are reported here. The temperature of the carbon material in these tests was 755 and 850 °C, respectively. For the experiment carried out at 755 °C, the temperature of sodium was varied from 600 to 700 °C with 50 °C intervals. For the experiment carried out at 850 °C, the temperature of sodium was varied from 600 to 750 °C with 50 °C intervals. The residence time at each sodium temperature was around 24 hours to ensure that equilibrium is reached. Measured temperatures at zone 2 are listed in Table I.

The carbon materials after the test were characterized by visual inspection and X-ray diffraction (Bruker AXS D8Focus, BRUKER). The surface area of the material was measured by a gas adsorption analyzer (TriStar II 3020, Micrometitics<sup>®</sup>), where N<sub>2</sub> was used as absorbent gas.

## Results

The weight gain of the carbon samples due to exposure to the sodium vapor at 755 and 850 °C respectively is shown in Figures 2 and 3. Sodium pressure, controlled by the temperature in zone 2 is listed in Table I.

Both the raw data and data corrected for the sodium uptake by the wire are shown in the figures. The thermogravimetric data demonstrate that sodium uptake increases with increasing sodium vapor pressure, and decreases with reducing sodium partial pressure. The weight response due to a change in the vapor pressure was relatively fast and equilibrium, corresponding to a constant weight, was obtained after a few hours.

Table I. Measured temperature at zone 2 as well as the corresponding sodium vapor pressure (calculated by Equation (3)) and activity. Number 1 to 7 is corresponding to labels in Figure 2 and 3.

	Temp. at zone 1: 755 °C			Temp. at zone 1: 850 °C		
	T <sub>Na</sub> , °C	p <sub>Na</sub> , mbar	a <sub>Na</sub>	T <sub>Na</sub> , °C	p <sub>Na</sub> , mbar	a <sub>Na</sub>
1	615	43	0.15	630	54	0.07
2	663	87	0.31	668	93	0.12
3	700	142	0.51	709	160	0.21
4	663	87	0.31	746	250	0.33
5	622	48	0.17	707	156	0.21
6	/	/	/	668	93	0.12
7	/	/	/	627	52	0.07

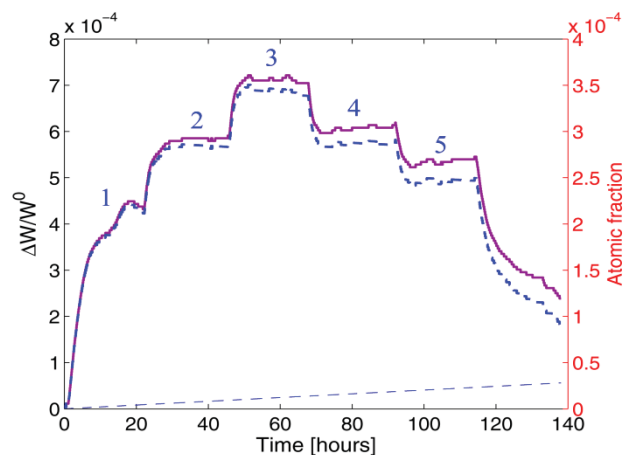


Figure 2. Weight gain [wt% and atomic fraction] of carbon at 755 °C as function of time and the vapor pressure of Na. Na vapor pressure was changed by changing Na temperature after about 24 h in the sequence listed in Table I. Bold solid line - experimental data. Bold dashed line - experimental data subtracted the weight gain of the wire (dashed line).

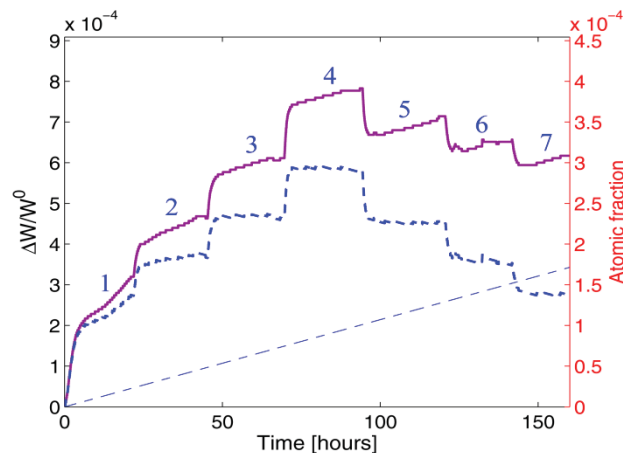


Figure 3. Weight gain [wt% and atomic fraction] of carbon at 850 °C as function of time and the vapor pressure of Na. Na vapor pressure was changed by changing the Na temperature after about 24 h in the sequence listed in Table I. Bold solid line - experimental data. Bold dashed line - experimental data subtracted the weight gain of the wire (dashed line).

The sodium uptake was quite limited in both cases and there were no visible change of the carbon sample after sodium exposure. X-

ray diffraction of the samples after the experiment (not shown) did not give any evidence of formation of new crystalline reaction products between sodium and carbon.

Optical images of the carbon exposed to sodium vapor and liquid sodium is shown in Figure 4. Unlike the case with sodium vapor, the exposure to liquid sodium caused severe disintegration of the sample, indicating a significant volume change due to the interaction with the sodium vapor. Despite the clear physical changes there could still not be observed and sign of new crystalline compounds by XRD. This implies the sodium intercalation compounds are unstable or not possible to detect by XRD.



Figure 4. Graphite sample after reaction with sodium vapor [left] and sodium liquid [right].

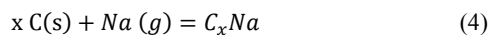
### Discussion

The weight change as a function of sodium partial pressure for the reported tests is shown in Figure 5. Both the results obtained during heating and cooling are shown in the figure. The sodium pressure, as a function of the vapor pressure was calculated by Equation (3) [18]:

$$\ln p = 11.9463 - 12633.73/T - 0.4672 \ln T \quad (3)$$

where  $T$  is temperature given in K and  $p$  is sodium vapor pressure given MPa.

The thermogravimetric data demonstrate that sodium uptake decreases with increasing temperature at the same sodium activity in the gas. The reaction between the sodium gas and carbon can be expressed as



The entropy of the reaction is clearly negative due to sodium gas at the left hand side and it is therefore expected that the concentration of sodium in carbon decreases with increasing temperature in line with the observations.

Mikhalev and Øye [9] treated the uptake of sodium as a BET isotherm [19]. The BET isotherm theory is related to the surface sorption and does not take intercalation or solubility of sodium atoms in the bulk graphite lattice into account. The general BET isotherm can be expressed as Equation (5)

$$\frac{p/p^0}{(\Delta W/W^0)(1-p/p^0)} = \frac{1}{C\Delta W_m/W^0} + \frac{(C-1)(p/p^0)}{C\Delta W_m/W^0} \quad (5)$$

where  $p$  is sodium vapor pressure,  $p^0$  is the vapor pressure of pure sodium,  $C$  is a constant,  $\Delta W_m$  is the weight of sodium in a

monolayer,  $W^0$  is the initial sample weight and  $\Delta W$  is the weight gain. The BET isotherm based on the experimental data from the present study is shown in Figure 6.

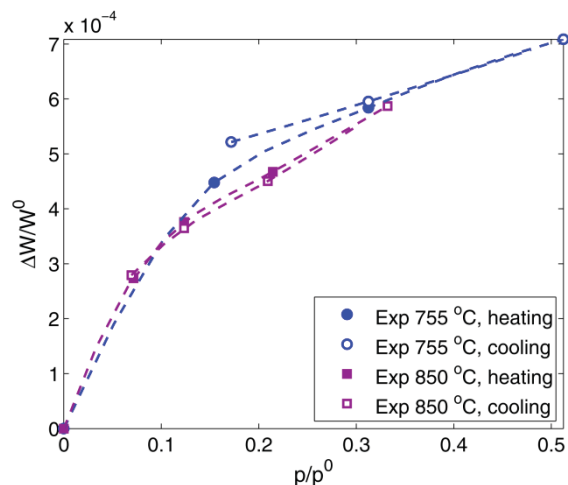


Figure 5. The relative amount of sodium in the carbon material as a function of the sodium partial pressure at 755 and 850 °C. The sodium vapor pressures ( $p^0$ ) at 755 and 850 °C are 278 and 755 mbar respectively

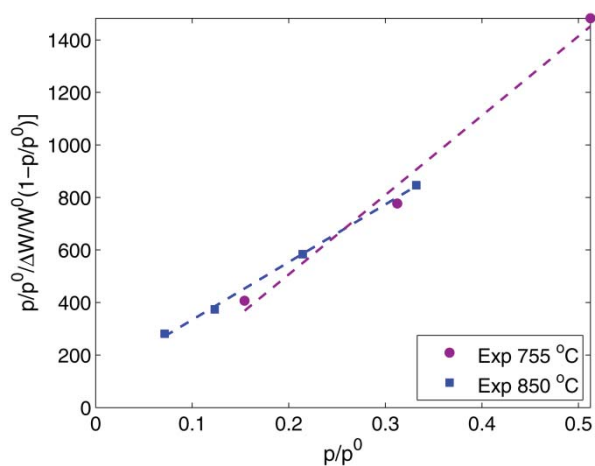


Figure 6. BET plot for carbon sample at 755 and 850 °C (carbon temperature), the dashed lines are linear fitting of the experimental data.

The calculated surface area based on BET plot in Figure 6 was 1.0 m<sup>2</sup>/g and 1.2 m<sup>2</sup>/g at 755 and 850 °C respectively. The measured surface area was 0.2 m<sup>2</sup>/g. Not surprisingly, the calculated surface areas by the BET approach is significantly larger than the N<sub>2</sub> experimental value. This trend was the same as reported previously by Mikhalev and Øye [9]. The reason is that the interaction between graphite and sodium and the interaction between graphite and N<sub>2</sub> gas are inherently different. The former involves surface adsorption and intercalation of sodium atoms into the graphite lattice. The latter is only the adsorption of gas molecules on the exposed graphite surface.

The compounds formed by sodium intercalation in the material could not be detected by XRD after the graphite sample had been exposed to sodium. The proposed reason is that the sodium intercalation compounds are in general energetically not favorable,

which has been elaborated in a recent DFT study of the energetics of alkali metal graphite intercalation compounds by Wang et al. [17].

The enthalpy of formation of intercalation compounds of sodium in graphite is shown in Figure 7.

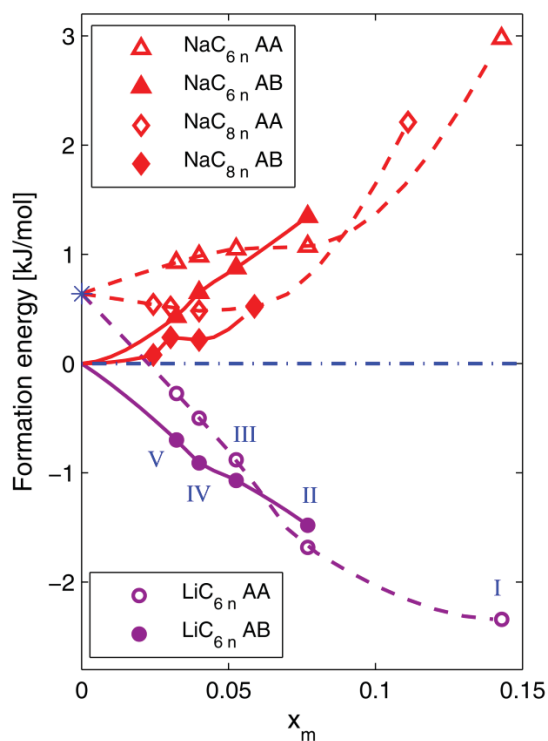


Figure 7. Formation energy of stoichiometric Li and Na graphite intercalation compounds (GICs). Composition given as mole fraction of alkali metal  $x_m$ . For example, for the first stage  $\text{LiC}_6$ ,  $n=1$ ,  $x = 1/(1+6n)=1/7$ . Stage I to V for Li-GICs is indicating in the figure.  $\text{MC}_x$  AA refers to AA stacking graphene layers between two adjacent alkali metal layers, while  $\text{MC}_x$  AB refers to AB stacking graphene layers between two adjacent alkali metal layers. “\*” in the figure refers to the difference of formation energy of artificial graphite with AA stacking sequence compared to graphite (with AB stacking).

Unlike lithium, the enthalpy of formation of sodium intercalation compounds is endothermic, which implies that the intercalation reaction, reaction (4), is energetically not favorable. This is also in agreement with the lack of evidence of the formation of lower stage intercalation compounds in carbon, only  $\text{NaC}_{64}$  has been reported [20]. This also explains the low sodium uptake observed by thermogravimetry, as shown in Figure 2 and 3. The sodium uptake would be enhanced by increasing sodium activity, such as in the case of direct contact with sodium liquid (high vapor pressure) or by an applied external electrical field. However, sodium in graphite could not persist in the graphite lattice due to its instability when the sodium activity decreases. The surface absorption was assumed to be much faster than lattice diffusion, and the relaxation was diffusion controlled.

A transient diffusion model implemented in COMSOL Multiphysics® 4.3 was used to simulate the thermogravimetric

relaxation curve. The transport of sodium into graphite was assumed to consist of two steps; adsorption of sodium at the surface and lattice diffusion from the surface into the bulk. The curve fitting shown in Figure 8 and 9, were prepared using the following assumptions:

The diffusion coefficient is only temperature dependent. Varying the boundary condition, initial surface concentration  $c_0$ , changes only the absolute value of the weight gain over time but not the time to reach equilibrium. Surface absorption is much faster than diffusion and it does not affect the time scale to reach equilibrium.

Based on the assumptions above, only part of the experimental relaxation curves is enough to derive the apparent diffusion coefficient of sodium vapor in graphite material. Surface adsorption does not need to be taken into consideration. In addition, the normalized weight gain would be more convenient for data fitting.

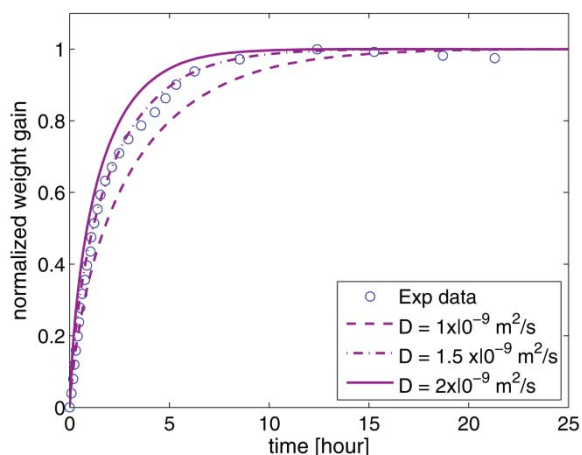


Figure 8. Normalized weight gain as a function of time for the thermogravimetric test at 755 °C. Lines are the simulated weight gain. Experimental data is shown for comparison. The data for sodium at 43 mbar from the test is used in the simulations.  $c_0$  is equal to  $1 \text{ mol/m}^3$ .

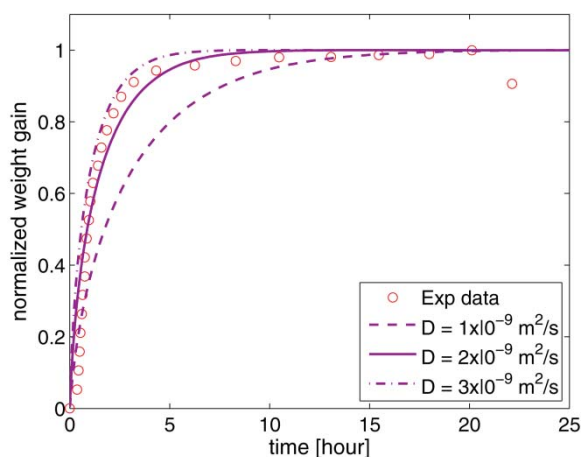


Figure 9. Normalized weight gain as a function of time for the thermogravimetric test at 850 °C. Lines are the simulated weight gain. Experimental data is shown for comparison. The data for sodium at 93 mbar from the test is used in the simulations.  $c_0$  is equal to  $1 \text{ mol/m}^3$ .

The simulations demonstrate that the relaxation time to reach equilibrium is very sensitive to the diffusion constant of sodium in carbon. The diffusion coefficient of sodium in graphite determined from the simulation was  $1.5 \times 10^{-9} \text{ m}^2/\text{s}$  at  $755 \text{ }^\circ\text{C}$  and  $2.5 \pm 0.5 \times 10^{-9} \text{ m}^2/\text{s}$  at  $850 \text{ }^\circ\text{C}$ . Extrapolating the data to  $960 \text{ }^\circ\text{C}$  gives a diffusion coefficient in the range  $4.5 \pm 1.5 \times 10^{-9} \text{ m}^2/\text{s}$ . The value is lower compared to the data from the Rapoport test of graphite material, which was reported by Ratvik et al. [8] to be  $3.22 \times 10^{-8} \text{ m}^2/\text{s}$ .

The diffusion coefficient derived by the simulation of the relaxation is the apparent overall diffusion coefficient, which has two contributions; diffusion of sodium (gas) through pores in the carbon material and lattice diffusion of sodium in graphite.

The FEM methodology was further used to simulate the entire weight curve by introducing the diffusion coefficient determined previously and the simulation is compared to the experimental data in Figure 10. The boundary conditions, initial surface concentration ( $c_0$ ) for the case study are listed in Table II. In this model, only diffusion is taken into account.

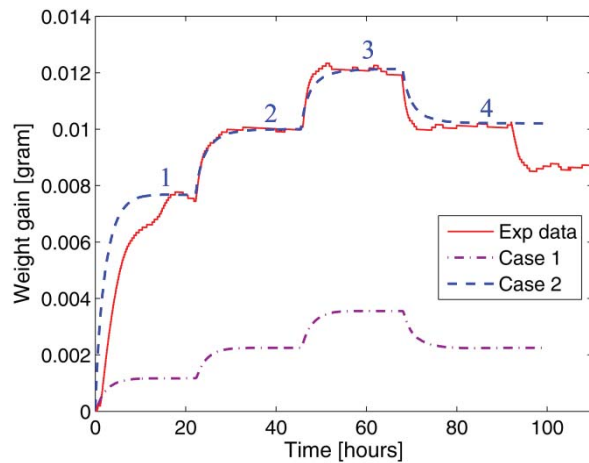


Figure 10. Simulated weight gain as a function of time by a diffusion model for the thermogravimetric test at  $755 \text{ }^\circ\text{C}$ . The boundary conditions, initial surface concentration ( $c_0$ ), in Case 1 and 2 listed in Table 2.

Table II. Boundary condition, initial surface concentration ( $c_0$ ), unit in  $[\text{mol}/\text{m}^3]$ . Number 1-4 corresponds to step 1-4 shown in Figure 10.

	Case 1	Case 2	Case 3
1	0.58	3.80	36.44
2	1.12	4.95	47.52
3	1.76	6.01	57.66
4	1.12	5.04	48.44

$c_0$  in Case 1 is derived from sodium vapor pressure, which is determined by the temperature of liquid sodium by Equation (3).  $c_0$  is then calculated by ideal gas law when its vapor pressure is known. The concentration in Case 1 is equal to the concentration of sodium in the gas phase. As shown in Figure 10, the calculated overall sodium uptake in the graphite sample is far too low to match the experimental data.

An alternative approach to estimate  $c_0$  is from the measured weight of sodium uptake in the graphite sample. The amount of weight gain divided by sample volume yields the average

concentration of sodium. By assuming the surface concentration is equal to the average concentration, and surface concentration reaches equilibrium at  $t=0$  due to the fast surface reaction,  $c_0$  can be estimated as the average concentration, which is listed as Case 3 in Table 2. In this case, the simulated sodium uptake is too high, which is not shown in Figure 10.

The best fitted concentration (Case 2) is around 10 times smaller than Case 3, see Table II. To determine the surface concentration correctly is still a challenge in this model. This was actually the same challenge as experience in a related study of sodium diffusion in cathode lining [21]. Therefore, a surface reaction which can relate the sodium in gas phase and the adsorbed sodium on graphite surface is needed to be coupled with the diffusion process in the simulation.

Figure 11 shows the preliminary simulation results from the model including surface reaction. In this model, the density of site for surface reaction is set to be  $1.5 \times 10^{-5} \text{ mol}/\text{m}^2$ , which is corresponding to 1 sodium atom having 2 coordinate carbon atoms on a graphite basal plane. The reaction rate is determined by rate of adsorption ( $r_{ads}$ ) and rate of desorption ( $r_{des}$ ), which are described as Equation (6) and (7) in the model:

$$r_{ads} = k_{ads} \times c_{Na,g} \times \theta_f \quad (6)$$

$$r_{des} = k_{des} \times \theta_{Na} \quad (7)$$

where  $k_{ads}$  and  $k_{des}$  are the adsorption and desorption rate constants,  $c_{Na,g}$  is the sodium concentration in gas phase,  $\theta_f$  is fraction of free site and  $\theta_{Na}$  is the surface coverage by sodium atom. In the present preliminary model  $k_{ads}$  is  $0.2 \text{ (m/s)}$  and  $k_{des}$  is  $0.5 \text{ mol}/(\text{m}^2\text{s})$ . These two rate constants are set in such a way that the surface reaction rate is much faster than the diffusion rate so that the process is diffusion controlled.

The challenge in this model is the difference between the “real” surface area and the geometric surface area. Normally, the simulation takes only the geometric surface into consideration, which is 1400 times smaller than the “real” surface area, in this case  $0.2 \text{ m}^2/\text{g}$  as discussed previously. Case 1 in Figure 11 is from the simulation based on geometry area, which is too low to match the experimental data. A scaling factor is necessary to transfer the geometry surface area to the “real” surface area of the material. A scaling factor 1400 is introduced in the model shown as Case 2 in the figure. The shape of this curve, however, could not match the experimental data well. To improve the fitting, a time dependent scaling function can be used. The reason is that the material is inhomogeneous and porous, and the “real” surface area is not exposed to sodium vapor at once when sodium vapor reaches the geometry surface but should increase gradually following the diffusion process. Further improvement of the simulation of the thermogravimetric relaxation data will be carried out in the future, but the preliminary work reported here shows that the present method is useful not only to determine the equilibrium sodium content in carbon as a function of the sodium activity but also the diffusion of sodium in carbon.

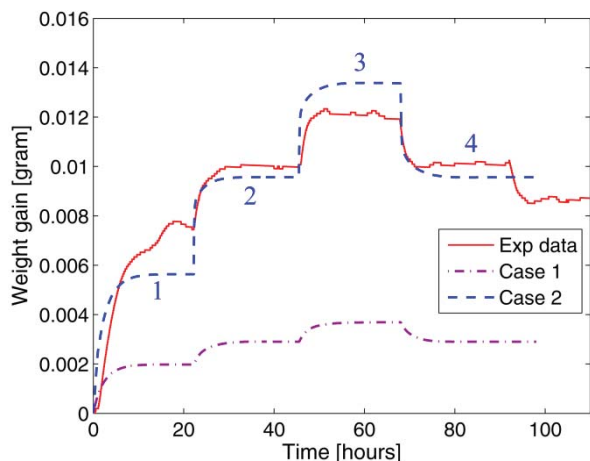


Figure 11. Simulated weight gain as a function of time by a combined diffusion and surface reaction model for the thermogravimetric test at 755 °C. Geometry surface area is applied in Case 1. “Real” surface area, 0.2 m<sup>2</sup>/g, is applied in Case 2 (sample weight: 17.6 g).

### Conclusion

The reaction between sodium vapor and graphite was studied by a thermogravimetric method. The equilibrium sodium content as well as the time to reach equilibrium after a change in the partial pressure of sodium at constant temperature were successfully determined by this method. The relaxation in the sodium content in carbon due to a change in the partial pressure of sodium was used to determine the sodium diffusion in carbon by a finite element method simulation. The diffusion coefficient of sodium in the graphite material was determined to be  $1.5 \times 10^{-9}$  m<sup>2</sup>/s at 755 °C and  $2.5 \pm 0.5 \times 10^{-9}$  m<sup>2</sup>/s at 850 °C. It can be concluded that the present method is suitable for investigation of the interaction between sodium and commercial carbon materials.

### Acknowledgement

The present work was carried out in the project “Durable Materials in Primary Aluminium Production” (DuraMat), financed by the Research of Norway, Hydro Primary Metal Technology, Sør-Norge Aluminium, and Elkem Carbon. Permission to publish the results is gratefully acknowledged.

### References

1. Siljan, O.J., C. Schøning, and T. Grande, *State-of-the-art alumino-silicate refractories for aluminium electrolysis cell*. JOM, 2002. **54**(5): p. 46-54;63.
2. Schøning, C. and T. Grande, *The stability of refractory oxides in sodium-rich environments*. JOM, 2006. **58**(2): p. 58-61.
3. Wang, Z., E. Skybakmoen, and T. Grande, *Spent Si<sub>3</sub>N<sub>4</sub> bonded SiC sidelining materials in aluminium electrolysis cells*. Light Metals (TMS), 2009: p. 353-358.
4. Wang, Z., E. Skybakmoen, and T. Grande, *Chemical degradation of Si<sub>3</sub>N<sub>4</sub> bonded SiC sidelining materials in aluminium electrolysis cells*. J. Am. Ceram. Soc., 2009. **92**(6): p. 1296-1302.

5. Sørli, M. and H.A. Øye, *Cathodes in Aluminium Electrolysis*. 3rd. ed. 2010, Germany: Aluminium-Verlag Marketing & Kommunikation GmbH.
6. Solheim, A. and C. Schøning, *Deterioration of the bottom lining in aluminium reduction cells - Part I: Chemical equilibria at 1100 K*, in *Aluminium of Siberia*. 2008: Knrasnoyarsk, Russia. p. 69-75.
7. Hop, J.G., *Sodium expansion and creep of cathode carbon*, in *Department of Material Science and Engineering*. 2003, Norwegian University of Science and Technology. p. 176.
8. Ratvik, A.P., et al., *The effect of current density on cathode expansion during start-up*. Light Metals (TMS), 2008: p. 973-978.
9. Mikhalev, Y. and H.A. Øye, *Absorption of metallic sodium in carbon cathode materials*. Carbon, 1996. **34**(1): p. 37-41.
10. Brisson, P.Y., et al., *The effect of sodium on the carbon lining of the aluminum electrolysis cell - a review*. Canadian Metallurgical Quarterly, 2005. **44**(2): p. 265-280.
11. Sangster, J., *C-Na (carbon - sodium) system*. Journal of Phase Equilibria and Diffusion, 2007. **28**(6): p. 571-579.
12. Rapoport, M.B. and V.N. Samoilenko, *Deformation of cathode blocks in aluminium baths during process of electrolysis*. Tsvetnye Metally, 1957. **30**(2): p. 44-51.
13. Kozlov, F.A., et al., *Study of the behavior of the graphite-sodium system for the central rotating column in a BN-600 reactor*. Atomic Energy, 2006. **101**(6): p. 887-893.
14. Zolochovsky, A., et al., *Rapoport-Samoilenko test for cathode carbon materials: I. Experimental results and constitutive modelling*. Carbon, 2003. **41**(3): p. 497-505.
15. Naas, T., *Interactions of alkali metals and electrolyte with cathode carbons*, in *Institutt for uorganisk kjemi*. 1997, Norwegian University of Science and Technology.
16. Houston, G.J., B.J. Welch, and D.J. Young, *Uptake of electrochemically generated forms of sodium by various carbons*. Light Metals (TMS), 1981: p. 529-540.
17. Wang, Z., S.M. Selbach, and T. Grande, *Van der Waals density functional study of the energetics of alkali metal intercalation in graphite*. PCCP, to be submitted, 2013.
18. Browning, P. and P.E. Potter, *An assessment of the experimentally determined vapour pressures of the liquid alkali metals, chapter 6.2 in Handbook of Thermodynamic and Transport Properties of Alkali Metals*. 1985.
19. Brunauer, S., P.H. Emmett, and E. Teller, *Adsorption of gases in multimolecular layers*. J. Am. Ceram. Soc., 1938. **60**(2): p. 309-319.
20. Asher, R.C., *A lamellar compound of sodium and graphite*. Journal of Inorganic and Nuclear Chemistry, 1959. **10**(3-4): p. 238-249.
21. Wang, Z., J. Rutlin, and T. Grande, *Sodium diffusion in cathode lining in aluminium electrolysis cells*. Light Metals (TMS), 2010: p. 841-847.